Rossby autosoliton and laboratory model of Jupiter's Great Red Spot

S. V. Antipov, M. V. Nezlin, E. N. Snezhkin, and A. S. Trubnikov
(Submitted 21 June 1985; resubmitted 18 July 1985)
Zh. Eksp. Teor. Fiz. **89**, 1905–1920 (December 1985)

A new nonlinear hydrodynamic structure has been observed experimentally: the Rossby autosoliton. It is an isolated vortex that, despite viscosity, is undamped and exists as a self-organized structure in axisymmetric zonal counter-flows in a rotating parabolic layer of "shallow water," in which it is maintained in a steady state by these flows. The vortex is identified as a Rossby soliton (a strongly nonlinear solitary wave) by the following criteria: It exists in a system with a meridional gradient of a Coriolis force, has a radius greater than the Rossby-Obukhov radius, is an anticyclone, and lags the global rotation of the system. The experimentally realized Rossby autosoliton can be regarded as a steady model of Jupiter's Great Red Spot, confirming qualitatively the soliton theory of this natural phenomenon. The autosoliton is generated by a centrifugal instability which arises in differentially rotating shallow water when the central part of the water has a more rapid rotation; under other experimental conditions, it simulates a mechanism of formation of galactic spiral structure. In contrast to the Red Spot model based on thermogyroconvection in "deep water," this soliton model gives a natural explanation for the drift of the natural vortices in the atmospheres of Jupiter and Saturn and their cyclonic-anticyclonic asymmetry. The model can be brought into good quantitative agreement with the data of Red Spot observations if the wave motion in not only the horizontal but also the vertical is taken into account.

1. INTRODUCTION

In the work reported in Refs. 1 and 2, we created experimentally for the first time and investigated a Rossby soliton in a model of a homogeneous planetary atmosphere realized in the form of a layer of "shallow water" with free surface, the layer rotating together with its vessel of parabolic shape. The Rossby soliton is a solitary nonlinear vortex. In the nonsustained regime, i.e., in the absence of external "pumping" (by, for example, the zonal counter-flows considered below), it keeps its shape for a time appreciably greater than the time of dispersion spreading of a linear wave packet of the same size (cf. Secs. 1 and 3). The vortex rotates in the Rossby regime, i.e., the frequency ω of its intrinsic rotation is small compared with the rotation frequency Ω_0 of the system as a whole:

$$\omega \ll \Omega_0. \tag{1}$$

The direction of rotation of the soliton is anticyclonic, i.e., the curl of its velocity is antiparallel to the vector $\mathbf{\Omega}_0$. The vortex is in a state of geostrophic equilibrium—the Coriolis force acting on the circular stream of particles around the vortex axis is equalized by the gradient of the hydrostatic pressure. Because of the presence of the so-called β effect (a dependence of the vertical component of $\mathbf{\Omega}_0$ on the meridional coordinate), the vortex drifts in the opposite direction to the rotation of the system as a whole. (The possible existence of such a soliton in a layer of shallow water rotating together with a vessel of parabolic shape was pointed out in the theoretical study in Ref. 3a.)

In its physical parameters and propagation properties (size, direction of the rotation and the drift, and the drift velocity), the Rossby soliton found and studied in Refs. 1 and 2 was qualitatively similar to the remarkable natural vortex in the Great Red Spot of Jupiter and can be regarded as a laboratory model of it, supporting qualitatively the soliton theory of this natural phenomenon.[3–6] However, this variant of the model had at that time an obvious shortcoming, in that the laboratory soliton was created by a localized source as a result of brief rotation of a "pumping disk" situated in the plane of the bottom of the vessel. The lifetime of the soliton formed after the excitation pulse was about 20 sec and was limited by the time of viscous damping. In the case of the Red Spot vortex, the characteristic time of viscous damping can be estimated at[7a]

$$\tau_{\text{visc}} \approx \pi H_0 (\nu \Omega_0)^{-1/2}, \tag{2}$$

where H_0 is the equivalent depth of the atmosphere, and ν is the kinematic viscosity; for $H_0 \approx 25$ km, $\nu \approx (1\text{–}2)$ cm^2/sec, and $\Omega_0 \approx 1.6 \cdot 10^{-4}$ sec^{-1} (the rotation period of the planet is ≈ 10 h), $\tau_{\text{visc}} \approx 10^1$ yr.[1)]

But the natural vortex of the Red Spot has already been observed without significant changes for about 300 years.[8] It is therefore clear that its steady state can be explained only by "sustenance" from outside. This function is most probably performed by the zonal counter-flows (shear), which give rise to winds along the parallels whose amplitude and direction vary along the meridian (Fig. 1); the instability of these flows evidently sustains the Red Spot vortex, compensating its viscous and, possibly, other momentum losses.[4–6] According to the theory of Refs. 9 and 10, the picture of zonal flows shown in Fig. 1 arises as the result of nonlinear evolution of two-dimensional turbulence in the atmospheres of rotating planets: Vortices combine subject to a restriction of the vortex scale along the meridian (the Rhines length (3) (Ref. 9) but with no restriction along the parallel, as a result of which closed zonal flows are formed, their direction changing sign periodically along the direction of the merid-

 0038-5646/85/121097-11$04.00

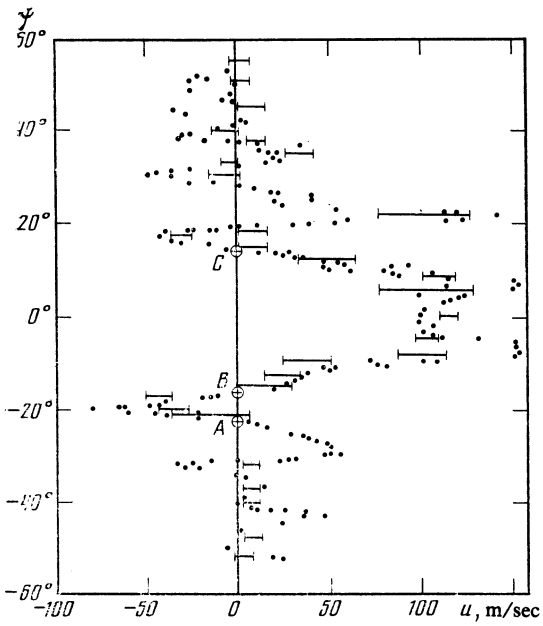

FIG. 1. Zonal flows in the upper atmosphere of Jupiter: wind velocity (m/sec) as a function of geographical latitude.[8c,8d] At the point A (at which the vorticity of the flows is anticyclonic) is the Red Spot vortex; at the point B (cyclonic vorticity) there is no vortex, while at the point C (cyclonic vorticity, velocity gradient of the wind several times greater than at the Red Spot) cyclonic "barges" exist.[20b,8b]

ian (see Fig. 1).

The width of these flows is

$$l \approx \pi (u/\beta)^{1/2}, \tag{3}$$

where u is the amplitude of the flow velocity, $\beta = (2\Omega_0/R)\cos\varphi$, R is the radius of the planet, and φ is the geographical latitude.

To give the soliton model properties closer to those of the Red Spot, it was natural to attempt to keep the soliton, having produced it by a local pulsed source (for example, by the same pumping disk), in a steady regime by the addition of zonal counter-flows around the vortex that can sustain it. We made such an experiment and obtained a negative result, namely, if the flows had a velocity sufficiently small for them not to be subject to intrinsic instability they broke up ahead of the soliton since their velocity profile did not correspond to that of the soliton. But if the velocity of the flows was sufficiently great, then (by the development of intrinsic instability) they generated several of their "own" vortices, ignoring the task put upon them of sustaining the single (initially specified) soliton.

Besides this negative result, the experiment did have a very positive consequence—it stimulated a program of experiments to study the stability of zonal flows, which was begun in Refs. 11 and 2 (see also Ref. 6b). This work showed that by means of zonal counter-flows in a rotating parabolic layer of shallow water one could already (without any additional local source) create steady trains of anticyclonic vortices—Rossby solitons. It was also found that the number of vortices in such a train that fit onto the perimeter of the system decreases with increasing velocity of the counter-flows, and this offered the prospect of the generation of low modes of the instability, including the first.

The decisive step was taken in the work reported here (see also the brief communication of Ref. 12). On the basis of the previous experimental equipment,[1,2] we made an experiment in which the distance between the flows and their velocity were greatly increased. This experiment led to the creation of the Rossby autosoliton—an anticyclonic vortex existing by *itself* on the complete perimeter of the system, formed from the unstable counter-flows and existing in a steady state under conditions of a smooth profile of the flows.[2)] The experiment is described and its results are analyzed in Sec. 2.

Further, in Sec. 3, we describe experimental data on the generation of steady *cyclonic* structures by counter-flows with a strong meridional gradient of the velocity; the cyclones corresponding to these structures are fundamentally different from the anticyclones—in the nonsustained regime they decay comparatively quickly because of dispersion, and their lifetime in our experiments is appreciably shorter than the time of dispersion spreading of a linear packet of Rossby waves, so that they are not solitons. The interpretation given for these results makes it possible to explain the existence of long-lived cyclonic structures in the atmosphere of Jupiter (as exceptions), and also in the Earth's atmosphere.

In Sec. 4, we consider manifestations of two different instabilities of zonal flows in rotating shallow water. As is shown by the experiment of Ref. 13 in accordance with the theory of Ref. 14, one of these instabilities, the analog of the classical Kelvin-Helmholtz instability, is stabilized (suppressed) if the jump in the flow velocity exceeds by a sufficiently large amount the characteristic velocity of waves on the shallow water. This fact, which is analogous to the suppression of the two-dimensional instability of a two-dimensional shear discontinuity in a compressible medium,[15] is a good illustration of the physical analogy between two-dimensional gas dynamics and shallow-water dynamics.[16] Another instability observed in differentially rotating shallow water is the centrifugal instability. It was predicted theoretically[17] for a differentially rotating thin galactic gas disk and has been identified experimentally for the case of shallow water in the simulation[18] of the hydrodynamic mechanism of generation of galactic spiral structure. The centrifugal instability, which develops if the central part of the medium rotates more rapidly than the periphery, persists even at the large values of the velocity jump for which the Kelvin-Helmholtz instability disappears. As the experiment shows, it is the development of the centrifugal instability in shallow water that leads to the formation of the Rossby autosoliton[12] and also simulates the mechanism of formation of spiral structures in the gas disks of galaxies.[18]

In Sec. 5, the soliton model of the Red Spot is considered with allowance for the fact that the wave motion of this natural vortex evidently has a three-dimensional nature, i.e., includes vertical oscillations. It is shown that in this way it is possible to improve the two-dimensional model[3)] (transforming it into a three-dimensional one) and obtain good qualitative agreement between the theoretical model and the observational data (see Ref. 6).

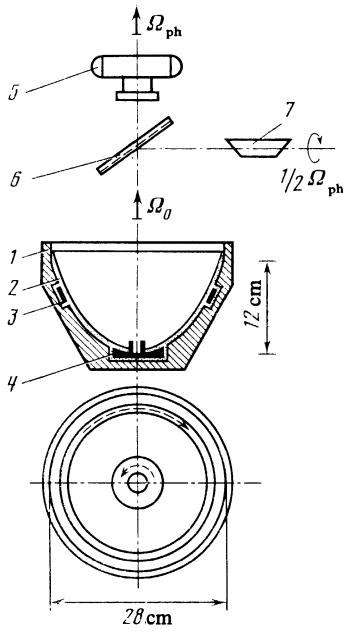

FIG. 2. Experimental arrangement: 1) vessel with nearly parabolic profile of the bottom rotating counterclockwise about the vertical axis; 2) water that spreads over the bottom of the paraboloid when it rotates; 3) and 4) rotating rings producing counter-flows with velocity shear; the directions of the arrows showing the flows as seen from above correspond to an anticyclonic shear; 5) camera with adjustable rotational velocity Ω_{ph}; 6) semitransparent mirror; 7) Dove prism of the rotoscope.

In Sec. 6, we consider the alternative model of the Red Spot and other atmospheric planetary vortices based on thermogyroconvection in deep water and compare it with the model developed in the present paper on the basis of the Rossby autosoliton in shallow water; the conclusion is drawn that, in our view, the soliton model is better and explains more fully the properties of these natural vortices.

2. THE ROSSBY AUTOSOLITON

The basis of the experiment is a vessel (Fig. 2) with an approximately parabolic profile of its bottom, diameter 28 cm, and depth 12 cm (for more details, see Refs. 12 and 2). The working liquid (water), which is distributed in a thin layer over the bottom of the vessel when it rotates, was subject to the effect of two counter-flows moving along the parallels around the axis of the system. The flows relative to the rotating vessel were produced by the differential motion of two sections of its bottom, which were displaced relative to the vessel in opposite directions and carried along the layers of liquid situated above them. The internal section consisted of the entire central part of the bottom with a diameter of 10 cm; the outer section, a ring of width 2.5 cm, was situated at a distance of 11 cm from the inner section (the last two distances are measured along the meridian of the paraboloid). Between them was a section of the paraboloid itself, rotating as a whole. The width of the gaps between the sections (0.5 mm) was much lesss than the working thickness of the liquid layer ($H_0 = 0.5$–1 cm).

The pattern of the flows and generated structures were made visible by white test particles floating on the surface of the water on the background of the black bottom of the vessel, and it was observed through a rotoscope constructed on the basis of a Dove prism. The rotation frequency f_1 of the prism and the corresponding rotation frequency of the coordinate system in which a cine film was made ($f_2 = 2f_1$) could be varied in a controlled manner independently of the rotation speed of the vessel. The photographing was done by means of a camera that rotated coaxially with the vessel, the rotation of the camera being synchronized with the rotation of the Dove prism in such a way that the obtained photographs were identical to the picture observed through the rotoscope. In these experiments, the camera rotated around the axis of the device together with the observed vortex, which drifted relative to the paraboloid in the opposite direction to its rotation. The main results of the experiment are as follows.

1. For the appreciable separation in this experiment of the counter-flows, their instability led, as in Refs. 12 and 2, to the generation of large-scale vortex structures (with scale greater than the Rossby-Obukhov radius determined below) only in the case of anticyclonic direction of the flows, when the curl of their velocity, the vorticity, is antiparallel to the

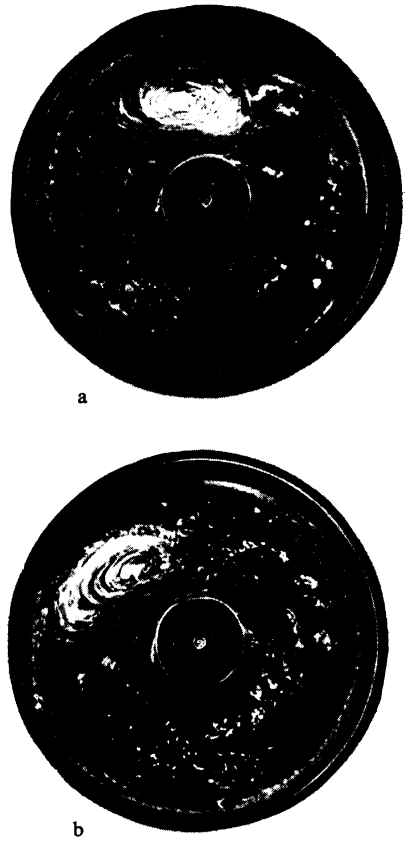

FIG. 3. Rossby autosoliton: examples of visualization for several different velocities of the counter-flows. The white lines are the tracks of test particles floating on the surface of the liquid on the background of the black bottom of the paraboloid; $\Omega_0 = 12.6\,\text{sec}^{-1}$, exposure 1/3 sec. The distance of the center of the vortex from the rotation axis is about 6 cm. The vortex rotates and drifts clockwise.

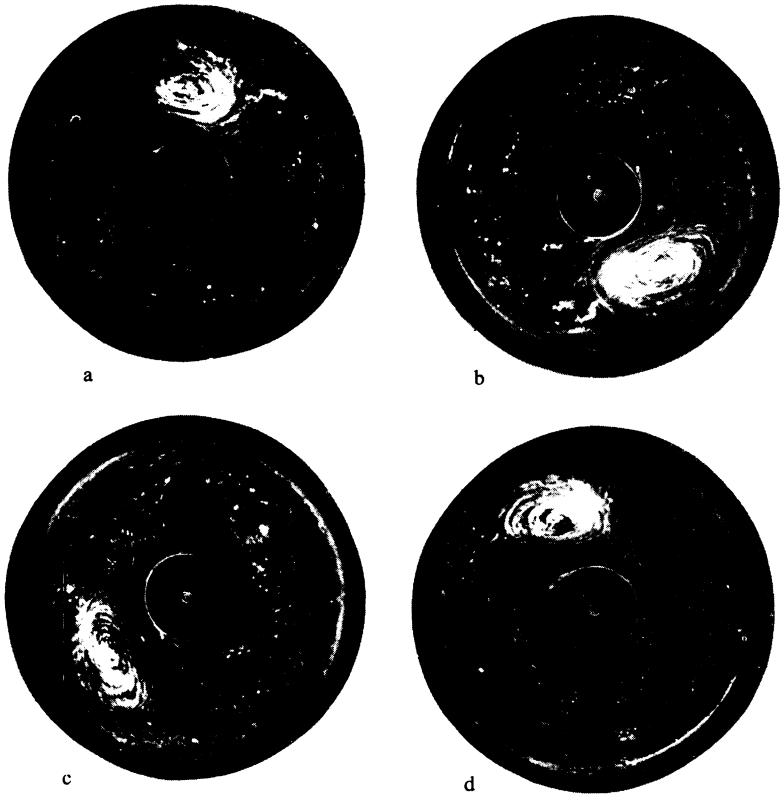

FIG. 4. Phases of the drift of the Rossby autosoliton in the opposite direction to the rotation of the vessel. The vessel rotates counterclockwise.

angular velocity vector of the paraboloid; but if the velocity curl of these (fairly widely spaced) flows is cyclonic, large-scale vortex structures are not generated. This cyclonic-anticyclonic asymmetry observed in a system with a pronounced β effect is a fundamental nonlinear property of Rossby vortices and is due to the fact that large anticyclones in the nonsustained regime can be Rossby solitons but large cyclones cannot—as the experiment of Refs. 1 and 2 showed, the cyclones decay comparatively quickly, since for them, in contrast to the anticyclones, the dispersion spreading is not compensated by nonlinearity.

2. Figure 3 shows the picture of the flows (of anticyclonic direction) and the vortex structure generated by them. The main element of this structure is the vortex of oval or approximately circular shape, which lags behind the global rotation of the paraboloid (i.e., it drifts in the opposite direction to this rotation—"to the west"). It is an anticyclone—the liquid rotating around the local axis in the direction opposite to the rotation of the vessel is elevated. The vortex exists for an arbitrarily long time, preserving its shape well (the limits of its spontaneous variation are illustrated by the example of Fig. 3). The photographs of Fig. 3 were taken by the camera rotating around the axis of the vessel with the same frequency with which the vortex rotates about the same axis (drifting relative to the paraboloid, the vortex is not displaced relative to the camera). The sequence of analogous photographs rotated relative to each other by the angle determined by the drift of the vortex during the time between the exposures demonstrates the different "phases" of its azimuthal motion with respect to the paraboloid (Fig. 4).

The dimensions of the vortex are 6–9 cm along the parallel and about 6 cm along the meridian, i.e., $(3–4)r_R$, where

$$r_R=(g^*H_0)^{1/2}/2\Omega_0\cos\alpha \qquad (4)$$

is the Rossby-Obukhov radius, g^* is the acceleration of the resultant of the force of gravity and the centrifugual force due to the global rotation, and α is the angle between the rotation axis of the system and the local normal to the equilibrium surface of the liquid in the absence of the flows. The vortex drift velocity V_{dr} is about 8 cm/sec and approximately twice the Rossby velocity corresponding to the "nominal" rotation frequency of the paraboloid, i.e., corresponding to constant thickness of the liquid layer (in the experiments, the rotation velocity of the vessel was somewhat greater than the nominal velocity). The Rossby velocity is determined by

$$V_R=g^*(\partial/\partial y)\,(H/f), \qquad (5)$$

where H is the depth of the liquid layer, $f=2\Omega_0\cos\alpha$ is the Coriolis parameter, and y is the coordinate measured along the median. In the paraboloid, $g^*=g/\cos\alpha$ and for $H=H_0=\text{const}$

$$V_R=\tfrac{1}{2}H_0\Omega_0\sin\alpha. \qquad (5')$$

We use here the relation (5), which differs from the expression given in Ref. 1b by having g^* taken in front of the differentiation symbol; the expressions (5) and (5′) are, as an analysis by A. V. Khutoretskiĭ and G. G. Sutyrin shows, more accurate. For a planet, there is hardly any difference

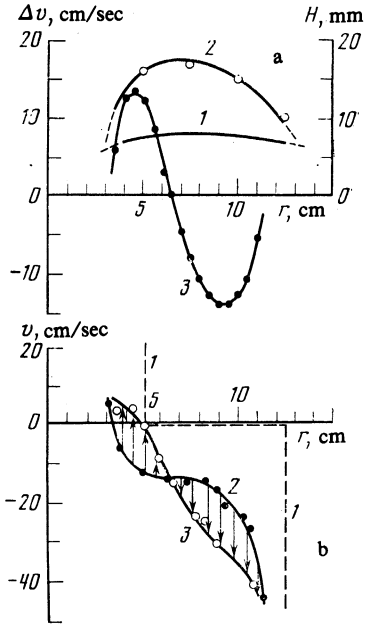

FIG. 5. a) Depth profiles of the liquid in the meridional section of the rotating paraboloid: the dependence of the depth of the liquid on the distance to the rotation axis (the depth is measured along the normal to the surface of the bottom at the given point) is the region exactly opposite the vortex (1) and in the region of the vortex (2); 3) the velocity profile within the vortex (the velocity is measured relative to the flow, as shown by the arrows in the lower figures). b) Profiles of the linear azimuthal velocity of the particles on the surface of the liquid in the frame of the rotating vessel. Dependence of the velocity on the distance to the axis of the vessel: 1) in the absence of the vortex, 2) in the vortex generation regime in the region exactly opposite the vortex, 3) within the vortex.

from Ref. 1b, since on a planet $g^* \approx g$, but in the case of the paraboloid (5') gives a Rossby velocity half that of Ref. 1b. It should also be noted that the use of (5') leads to much better agreement between experiment and theory (see Refs. 1 and 2).

The amplitude ΔH of the elevation of the vortex above the surface of the liquid (compared with the level of the surface of the liquid on the opposite side of the vessel), determined from the condition of geostrophic equilibrium,[1,2] is somewhat less than 1 cm, i.e., $\Delta H / H_0 \approx 1$ is somewhat greater than in the experiments of Refs. 1 and 2.

These properties of the vortex permit its identification as a Rossby soliton. (In connection with the group of questions discussed here, it is helpful to draw attention to the interesting theoretical study of Ref. 19.)

3. Figure 5a shows the profiles of the height of the liquid: 1) outside the vortex (on the side of the vessel opposite to it), 2) within the vortex. Figure 5b shows the velocity profiles in the vortex and in the flows. It can be seen that the vortex, which arises because of the instability of the axisymmetric counter-flows, radically changes their profile. Whereas the flow profile had the form of the step function 1 before the formation of the vortex, in the regime with it this profile has the form of the smooth curve 2. The velocity profile in the vortex itself is shown by the two curves 3 in Fig. 5; in the case of Fig. 5a, the velocities of the particles in the vortex (denoted by Δv) are measured relative to the flow, as is shown in Fig. 5b by the arrows between curves 2 and 3 (as positive direction of the velocity, the direction of the rotation of the system is taken). It is readily seen that the flows with the new profile are consistent with the spatial structure of the vortex and sustain its steady state, "twisting" the vortex and compensating its viscous (and, possibly, other) losses.

4. The maximal velocity of the local rotation of the liquid in the vortex (see curve 3 in Fig. 5a) is about 15 cm/sec and appreciably exceeds its drift velocity, this in fact corresponding to the presence in the vortex of a clearly defined region of trapped particles, as can be clearly seen in Fig. 3 (in this connection, see Ref. 1b). The maximal vorticity, the velocity curl of the vortex, appreciably (by 5–6 times) exceeds the vorticity outside the vortex (on the opposite side of the vessel), just as is observed in large vortices in the atmospheres of the planets.[20a]

Thus, the Rossby vortex created in the present study has all the characteristic properties of the Rossby soliton that we observed earlier in Refs. 1 and 2 and has in addition three new properties of a fundamental nature: First, despite the presence of viscosity (and other possible dissipation mechanisms), the vortex exists for an arbitrarily long time, i.e., it is an autosoliton. Second, like the large vortices in the atmospheres of the giant planets,[6b] it is not an element of a closed train of vortices but is a solitary formation, the only one on the entire perimeter of the system. Third, its creation does not require a special source—the autosoliton is generated by the nonlinear evolution of unstable axisymmetric counter-flows in rotating shallow water and rearranges their spatial profile in such a way that the new profile corresponds to a steady structure of the generated soliton. In other words, the autosoliton is the result of nonlinear self-organization of a Rossby soliton in a system of zonal counter-flows. It can be regarded as a realization of a steady laboratory model of the Great Red Spot, lending strong support to the soliton theory[3–6] of this natural phenomenon.

Our next task is to identify the instability that generates the Rossby autosoliton. The experimental data considered in Secs. 3 and 4 will help us to understand the nature of this instability.

3. CYCLONIC STRUCTURES

The question of the nature of the instability that gives rise to the anticyclonic vortex—the Rossby autosoliton—is intimately related to another question—that of the generation in our experiments of steady cyclonic structures physically similar to the so-called White Ovals (or "barges") observed in the northern hemisphere of Jupiter at 14° northern latitude.[20b] These are elongated cyclonic vortices measuring about 7.5 thousand kilometers along the parallel and not more than 1.5 thousand kilometers along the meridian. Despite the fact that these vortices pulsate strongly in time, they already exist not less than several tens of years and are the only exception to the rule according to which all the long-lived vortices observed on the giant planets are anticyclones.[6b,10b]

Our experiments (see, for example, Ref. 13) showed

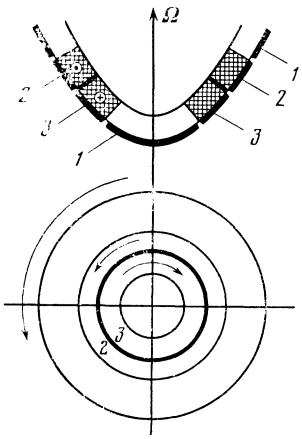

FIG. 6. Arrangement of experiment with a shear discontinuity: 1) bottom of vessel with paraboloidal bottom, 2) and 3) rings rotating in opposite directions relative to the paraboloid (seen from above, the directions of the arrows correspond to a cyclonic shear). The layers of water resting on the rings are hatched.

that by means of unstable counter-flows it is possible to generate steady trains of large-scale cyclonic vortices with dimensions exceeding r_R despite the fact that, as already pointed out above, solitary cyclones with such dimensions (in contrast to the anticyclones) decay comparatively rapidly in the nonsustained regime. Such generation of steady cyclonic structures is realized in the experiment illustrated schematically in Fig. 6. In this scheme, in contrast to the scheme of Fig. 2, the flows have the cyclonic sign of the vorticity (the angular velocity of the exterior flow is greater than that of the interior) and, which is particularly important, they are as close together as possible, namely, the width of the jump Δ in the velocity, i.e., the characteristic linear scale over which the change in the velocity occurs, is only a few millimeters (since $\Delta \approx H_0$), and this is much less than r_R. The configuration of Fig. 6 can be called a shear discontinuity. For this geometry of the experiment, the instability of the flows is manifested so rapidly that its growth rate exceeds the decay rate of the cyclonic vortices (including the decay rate of their viscous damping), and steady cyclonic structures are generated. Figure 7 shows one of the examples of such structures—a train of four cyclones (azimuthal mode $m = 4$) drifting in the direction of the global rotation of the paraboloid. The diameter 2a of these vortices is several times the radius r_R and large compared with H_0. As in the case of the previously described autosoliton, the number m of vortices on the perimeter decreases with increasing relative velocity of the flows (see below).

The experimentally observed basic difference in the efficiency of the generation of the cyclones and Rossby anticyclones can be explained as follows. Under the conditions of a "shear discontinuity" between the counter-flows, when

$$\Delta < r_R, \tag{6a}$$

the growth rate of the instability of the flows with respect to the generation of a train of vortices with period $\lambda > \Delta$ can be estimated approximately as[21]

$$\gamma \leqslant \gamma_{max} = \pi u/\lambda, \tag{6b}$$

where u is the velocity of the flows. When $u \gtrsim V_R$, $\lambda \lesssim 2\pi r_R$ this growth rate certainly exceeds the decay rate of the dispersion spreading of the cyclones, which is determined by the characteristic dispersion time[22]

$$\gamma_D = 1/\tau_D \leqslant V_R/8r_R. \tag{7}$$

Therefore, under the conditions of the shear discontinuity the counter-flows can even generate steady cyclones despite the fact that in the absence of the flows the cyclones decay comparatively quickly. (After the formation of the vortices, the velocity profile of the counter-flows becomes smoother, the growth rate of the cyclones falls, and as a result a steady state is established in which there is an equilibrium between the excitation of the vortices by the flows and their damping or decay.) But if the flow profile is smooth from the beginning, i.e.,

$$\Delta > r_R, \tag{8a}$$

then the growth rate of the instability of the flows with respect to the generation of vortices whose dimensions are comparable to (albeit larger than) r_R is greatly reduced[21,23]:

$$\gamma \ll \pi u/\lambda. \tag{8b}$$

At the same time, the condition $\gamma > \gamma_D$ for the excitation of cyclones ceases to be satisfied, and accordingly large-scale cyclones are not generated under the conditions (8a).

With regard to the (anticyclonic) Rossby solitons, they, as long-lived (nondispersive) formations,[1,2] are sustained in a steady state by the flows even under the conditions (8a).

In our view, it is just such a situation that obtains in the atmospheres of Jupiter and Saturn.[6b,10b] The vortex of the Red Spot and all the other long-lived vortices in the atmospheres of these planets (apart from Jupiter's "barges") are anticyclones; they are generated by zonal flows with smooth meridional velocity gradient corresponding to the condition (8a). But with regard to the cyclonic "barges" (Jupiter, 14° northern latitude), they are excited by (cyclonic) flows sa-

FIG. 7. Example of the generation of steady cyclonic structures in the case of a pronounced velocity profile of the zonal counter-flows[13] (in the geometry of Fig. 6). The white circle passing through the centers of the vortices is the line of the velocity "discontinuity" of the counter-flows.

FIG. 8. Example of the generation of steady anticyclonic structures under the conditions of the geometry of Fig. 6.

tisfying the relation (6a)—for them, the meridional velocity gradient is several times greater than at the Red Spot, and Δ is accordingly several times smaller.[20b]

This, in our view, is the interpretation of the pronounced cyclonic-anticyclonic asymmetry observed both in the experiments (Refs. 1, 2, 11, and 12) as well as in the atmospheres of the giant planets.[6b,10b] A distinctive feature of these planets is the smallness of the ratio of the radius r_R to the radius R of the planet; on Jupiter and Saturn $r_R \approx 6000$ km and $R \approx 70\,000$ km, and accordingly the regime (8a) can be realized on them. In contrast, in the atmosphere of the Earth, where $r_R \approx 3000$ km and $R \approx 6400$ km, the regime (6a), corresponding to Jupiter's "barges" (White Ovals),[20b] is almost always realized. Therefore, under terrestrial conditions the large planetary vortices can be either anticyclones or cyclones—everything depends on the sign of the vorticity of the flows that excite these vortices. (In addition, for the reasons given above, the vortices of the Earth's atmosphere, which are not large compared with the radius r_R, need not be Rossby vortices; see Ref. 25.)

4. NATURE OF THE INSTABILITIES THAT GENERATE ROSSBY VORTICES

We now show how the steady cyclonic structures described in Sec. 3 and the Rossby autosoliton described in Sec. 2 are generated by two different instabilities.

In our Ref. 13, we showed that cyclonic structures of the type of Fig. 7 are generated under the conditions of the geometry of Fig. 6 only when the magnitude of the jump at the shear discontinuity of the flows satisfies the condition

$$\Delta u \leqslant 2\sqrt{2}(g^* H_0)^{1/2}. \tag{9}$$

The experiment also shows that if under the condition (9) the sign of the vorticity of the counter-flows is reversed then the generation of steady anticyclonic structures occurs. They differ from the trains of cyclones described above by the sign of their vorticity and the drift (with velocity close to V_R) in the opposite direction to the global rotation of the system. An example of such a structure is shown in Fig. 8.

But if the jump in the velocity at the shear discontinuity exceeds the quantity on the right-hand side of (9), namely,

$$\Delta u \geqslant 2\sqrt{2}(g^* H_0)^{1/2}, \tag{10}$$

then, in accordance with the thoery of Ref. 14, there are no cyclonic structures and the flows are macroscopically laminar, i.e., do not generate large vortices with dimensions appreciably greater than the thickness of the layer of shallow water. This fact is illustrated by Fig. 9, which shows the suppression of the generation of the large cyclones when the condition (10) is satisfied and their appearance when the jump in the velocity across the shear is reduced from large values to the excitation threshold (9).

It is easy to see that the condition (10) is analogous to the condition for stability of a shear discontinuity in a homogeneous compressible medium with respect to two-dimensional perturbations perpendicular to the plane of the discontinuity[15]:

$$\Delta u \geqslant 2\sqrt{2} c_s, \tag{11}$$

where c_s is the velocity of sound.

The conditions (10) and (11) become identical if we make the substitution

$$c_s \to (g^* H_0)^{1/2}. \tag{12}$$

This is one of the manifestations of the analogy between two-dimensional gas dynamics and the dynamics of shallow water with a free surface: Gravity waves on incompressible shallow water, i.e., the raising and lowering of its surface, propagating with characteristic velocity $(g^* H_0)^{1/2}$, are physically equivalent to sound waves in an actually compressible two-dimensional gas-dynamical medium.[16] (It is here appropriate to note that the existence of this analogy makes it possible, by means of experiments on differentially rotating shallow water—under conditions of a different geometry—to demonstrate the mechanism of generation of spiral structure in the gas disks of galaxies with an analogous rotation profile.[18])

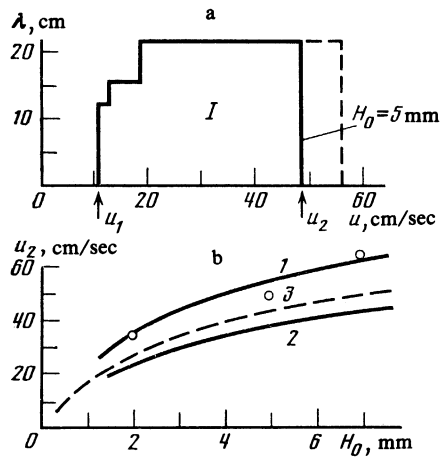

FIG. 9. Stabilization of shear-discontinuity instability in the case of cyclonic vorticity of the flows[13]: a) dependence of the azimuthal scale of the vortices on the velocities of the flows measured at the discontinuity on the surface of the water (I is the region of the instability); b) dependence of the threshold u_2 of stabilization of the shear-discontinuity instability on the depth of the liquid: 1) velocity of the rings. 2) velocity of the flows on the surface of the water, 3) theoretical velocity $(2g^* H_0)^{1/2}$. The broken curve shows the instability threshold for increasing flow velocity.

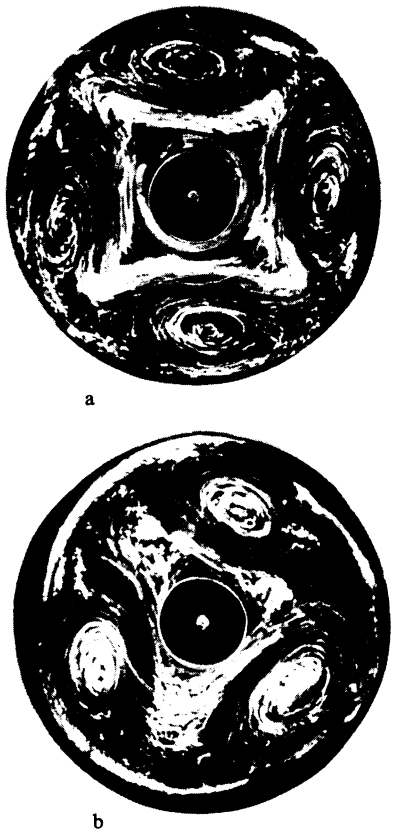

FIG. 10. Trains of autosolitons: the modes $m = 4$ (a) and $m = 3$ (b).

In establishing the similarity between the stability condition (10) of the considered shallow water configuration and the Landau stability condition (11), we must also note one fundamental difference. It is due to the fact that the condition (11) is derived for a flat discontinuity, whereas here we consider experiments with rotating shallow water and, accordingly, curvilinear discontinuities. This difference leads to a new feature: As the experiment shows, the suppression of the instability of the shear discontinuity (the Kelvin-Helmholtz instability) occurs in the system shown in Fig. 6 only when the angular velocity of the rotation of the system increases toward the periphery; in other words, when the vorticity of the flows is cyclonic, i.e., coincides with the direction of the angular velocity vector of the system. For the opposite (anticyclonic) vorticity of the counter-flows, an increase in their relative velocity merely leads to successive replacement of the azimuthal modes of the instability—the higher the velocity, the lower the mode number.[11,2] A similar behavior is observed when the flows are sufficiently far apart, i.e., under the conditions of Figs. 2 and 3. As examples, Fig. 10 shows pictures of the $m = 4$ and $m = 3$ modes of the instability observed at velocities of the exterior flow equal to $u = 200$ cm/sec and $u = 250$ cm/sec. Figure 11 shows the sequence of alternations of the azimuthal modes of the instability with increasing velocity of the exterior flow in the geometry of Figs. 2 and 3. In this geometry, generation of the Rossby autosoliton ($m = 1$) is observed when the velocity of the counter-flows is sufficiently great. This occurs when the velocity of the outer ring (producing the exterior flow) is ~350 cm/sec, i.e., at Mach number

$$\mathrm{Ma} \equiv u (g^* H_0)^{-1/2} \approx 8 \gg 2\sqrt{2}, \qquad (13)$$

when the "cyclonic" Kelvin-Helmholtz instability described above is absent (see also the end of Sec. 5). The result (13) and the alternation of the azimuthal modes of the instability (analogous to what is observed when spiral waves are generated on shallow water[18]) indicate that the Rossby autosoliton is generated by the centrifugal instability of the differentially rotating liquid.[18] So it must in accordance with the theory of Ref. 17b, which takes into account the small but finite width of the jump in the velocity at the "shear discontinuity." The centrifugal instability develops when the rotational angular velocity of the system decreases (sufficiently rapidly) toward the periphery; under appropriate experimental conditions, it simulates the hydrodynamic mechanism of formation of galactic spiral structure.[18]

We note that the difference between the pattern of the vortices observed in the present work and in Refs. 11, 12, and 2 from the pattern of spiral waves[18] generated by the same instability is due to the fact that the vortices are observed in the actual region of the velocity gradient of the flows, whereas the spirals are observed far from it.

We must here consider the question why the observed structures are Rossby vortices. The point is that vortex trains superficially similar to those shown here (Figs. 7, 8, and 10) are also observed in entirely different experimental situations that either have no relation to the Rossby regime (1) at all or, at least, to the regime of generation of Rossby vortices. We give some examples. One of them is the experimental study of Ref. 24 of the Kelvin-Helmholtz instability in counterstreaming concentric gas jets. By the design of the authors, this was done under conditions for which the counter-flows are symmetric with respect to the laboratory frame of reference, which, thus, is inertial; therefore, the inertial forces (centrifugal and Coriolis) can be ignored, and, therefore, the regime of the experiments of Ref. 24 is not the Rossby regime. Accordingly, the β effect is also absent in these experiments. In addition, in Ref. 24 the Mach number $\mathrm{Ma} \to 0$. Very effective generation of vortex trains is demonstrated in Ref. 25, which simulate the polar cyclones on the

FIG. 11. Alternation of instability modes (m) with variation in the velocity of the outer ring (in the geometry of Fig. 2) producing the outer flow. The arrows in the graph indicate the direction in which the velocity of the ring is changing.

Earth. In them, counter-flows are produced by the action of the Coriolis force on the forced pumping of water through a rotating annular layer with horizontal bottom. The most effective generation of steady vortices occurs under the conditions when the liquid is forced along the edges of the annular gap and flows together in the middle (where, thus, eddies are formed); it is readily seen that for such a direction of the motions cyclones are generated. In this system, a significant β effect is absent (the vortices have hardly any dispersion) (see the photographs).

In contrast to these experiments of Refs. 24 and 25, in our experiments we observe a significant influence of dispersion (β effect) on the properties of vortices of opposite signs, and this leads to such a pronounced nonlinear effect as the cyclonic-anticyclonic asymmetry in the Rossby regime; moreover, a pronounced asymmetry is also observed when the conditions of generation of the vortices of opposite signs are (in contrast to the conditions of Ref. 25) the same but the vortices have different lifetimes, the cyclones dispersing comparatively quickly. In addition, in contrast to Ref. 25, in which the vortex dimensions satisfy $a < r_R$, for the vortices observed in our experiments $a > r_R$.

5. THREE-DIMENSIONAL (QUASITWO-DIMENSIONAL) SOLITON MODEL OF THE RED SPOT

Thus, we have considered two instabilities of rotating shallow water that qualitatively simulate in a two-dimensional system the mechanism of formation of global vortices in the atmospheres of large planets; above all, we have considered the soliton conception of the natural vortex in the Great Red Spot. It is now natural to attempt a quantitative comparison of the two-dimensional soliton model of the Red Spot[3a] and the data of astronomical observations. Such a comparison, made in Ref. 6, gives the following results. It is found that the ratios of the observed values of the drift velocity of the vortex, V_{dr}, the frequency ω of its rotation about the axis, and the dimension a of the vortex to the theoretical values are

$$\sim 1/50 \text{ for } V_{dr},\ \sim 30 \text{ for } \omega \text{ and } \sim 1/6 \text{ for } a. \qquad (14)$$

It can be seen that there are very appreciable deviations of the predictions of the two-dimensional theory from the observational data, the deviations, moreover, being in different directions.

In an attempt to "reconcile" our soliton conception with the observations, we now take into the fact that the real vortex of the Red Spot is, from the wave point of view, strictly speaking a three-dimensional and not a two-dimensional formation. For it is formed in an atmosphere in which the density is not constant at different heights, decreasing with increasing height in accordance with a law intermediate between the adiabatic and the isothermal.[26] Under these conditions, vertical oscillations can take place in the vortex (as in a medium stable with respect to vertical convection). These oscillations can be taken into account (at the level of linear Rossby waves) in just the same way as is done for synoptic Rossby vortices in the ocean.[27] In this case it is found that the dispersion relation for the Rossby waves remains unchanged as regards its structure but instead of the "two-dimensional" Rossby-Obukhov radius r_R determined by (4) it contains the "three-dimensional" Rossby radius r_i, which depends on the well-known Väisälä-Brunt frequency of the vertical oscillations of a fluid stable with respect to convection. As in Ref. 27, but now not for the ocean but an isothermal atmosphere, as shown in Ref. 6, we obtain

$$\begin{aligned} r_i/r_R &= \frac{1}{\pi}\left[(\gamma-1)/\gamma\right]^{1/2} \approx {}^1/_6, \\ V_{R_3}/V_{R_2} &= (r_i/r_R)^2 = {}^1/_{36}, \\ \omega_3/\omega_2 &= (r_R/r_i)^2 = 36, \end{aligned} \qquad (15)$$

where the subscripts 2 and 3 relate to the two- and three-dimensional cases, respectively. These relations are written down for the first vertical mode of the oscillations: $k_z = \pi/H_0$. Following Ref. 6, we now assume that a three-dimensional soliton solution analogous to the considered two-dimensional solution but differing from it by the replacement of r_R by r_i exists. This assumption is justified fairly rigorously in the theoretical study of Ref. 28. Assuming for the parameters of the required soliton the relations (15) and comparing them with (14), we conclude that this soliton model can be brought into good quantitative agreement with the observations if the two-dimensional model of Ref. 3a is augmented (in the indicated manner) by taking into account the three-dimensionality of the wave motion. Perfected in this manner, the model should evidently be described as a quasi-two-dimensional rather than a three-dimensional model.

Taking into account this result, i.e., knowing the quantitative corrections, we restricted ourselves in the experiments described above with the Rossby autosoliton to the construction of a two-dimensional model of Jupiter's Red Spot, demonstrating all the qualitative properties of this natural vortex.

In speaking of a comparison of our model with the properties of natural vortices, it is important to consider the question of the value of the Mach number in our experiments in which stationary Rossby vortices are generated by counter-flows. Experiments in which the basic parameters and the geometry of the flows were varied in three forms of the experimental equipment (see above and Refs. 11–13 and 2) showed that the relative velocity u of the flows needed for excitation of a train of vortices of a given mode m increases with increasing Ω_0, H_0, and distance L between the flows (see Fig. 2). This corresponds to the following relationship: The difference of the flow velocities over the vortex scale (ua/L) must ensure a rotation velocity of the vortex appreciably exceeding the drift velocity, which is $\sim V_R$. It is under such a condition that we see a vortex with a well-defined region in which particles are captured (see Fig. 3). This relationship has the form

$$u \approx C V_R L/r_R \approx C\Omega_0^2 L (H_0/g^*)^{1/2}, \qquad (16)$$

where the coefficient C is of the order of a few units and depends on some details of the experiment. This relationship leads to a fairly large Mach number under the geometrical conditions of our work (see Sec. 4). It must however be recalled that in considering natural vortices we take into account quantitative corrections associated with the three-di-

mensionality of the wave motion (Sec. 5); the Ma, which in accordance with (16) is proportional to V_R, is reduced in accordance with (15) by several tens of times and thus can be reconciled with the value of Ma corresponding to natural conditions (for which Ma$\ll$1 always).

To conclude this section, we note a further interesting fact: In the oceans of the Earth there are observed to be monopole anticyclonic Rossby vortices—long-lived localized structures that form at the boundary of layers with several different densities and have the form of "lenses." Their characteristic scale somewhat exceeds the internal Rossby radius, and they are characterized by a pronounced cyclonic-anticyclonic asymmetry. These vortices (which exist at a depth of a few hundred meters from the surface of the ocean) can be regarded as "internal" Rossby solitons (see Refs. 19, 27, and 29).

6. ALTERNATIVE MODEL

We now consider the alternative model of global vortices in the atmospheres of the giant planets advanced by Hide and his collaborators.[30] This model is constructed on the basis of thermal convection in a rotating liquid and has been studied in small devices constructed as follows. In a liquid enclosed in the space between cylinders rotating around a vertical axis and having a horizontal bottom, a controllable radial temperature gradient is produced, this giving rise to a definite density gradient (of the order of fractions of a percent). This gradient, being noncollinear with the acceleration due to gravity, produces in the liquid a flow—a so-called thermal wind,[30,7] which has an azimuthal direction. If the temperature of the liquid (and with it the density) has a nonmonotonic radial variation, i.e., the density gradient changes sign somewhere in the gap, counter-flows develop in the liquid. They have either cyclonic or anticyclonic vorticity, this depending on the nature of the density extremum (maximum or minimum). The experiment of Ref. 30 showed that under certain conditions the flows become unstable in such a device and generate trains of vortices with different mode numbers. It is possible to choose conditions for which the liquid has a minimum of its density in the middle of the gap (i.e., the temperature is maximal there) and the mode $m = 1$ is generated, just one anticyclone existing on the perimeter of the system (though, it is true, a weak cyclone can be seen ahead of it).[30] Such a vortex structure is proposed in Ref. 30 as a model of the Red Spot. In the experiment of Ref. 30, a density extremum of the opposite sign (maximum of the density and, accordingly, minimum of the temperature) could not be created, and the corresponding situation was calculated numerically on a computer. According to the calculation, a structure of the type of the cyclonic barges on Jupiter must arise.

This model differs very appreciably from the soliton model considered above. Its main differences are as follows. 1. The horizontal scales of the vortices (like the gap between the cylinders) is appreciably less than the depth of the liquid; in other words, we are, by definition, dealing with "deep water." Such a situation evidently differs very significantly from the natural conditions on the planets. Thus, in the case of the Red Spot the horizontal scale of the vortex probably exceeds the vertical by three orders of magnitude. 2. The generated vortices do not have dispersion and hardly move relative to the vessel, so that the observed drift of the planetary vortices is not explained. 3. The pronounced cyclonic-anticyclonic asymmetry is also not explained. 4. If the properties of the Red Spot vortex are to be interpreted on the basis of this model, it is necessary to assume that at the center of the Red Spot there is a maximum of the temperature (minimum of the density), but this is in qualitative disagreement with the observational data—in the Red Spot vortex there is a minimum of the temperature (Ref. 26). 5. The vortex scales are much less than the "two-dimensional" Rossby-Obukhov radius and are approximately equal to the "three-dimensional" Rossby radius r_i. 6. For this model, allowance for the compressibility of the medium is fundamental.

However, despite these differences,the model has certain features similar to those of the soliton model considered above. First, in both models self-organized vortices arise through the instability of zonal counter-flows (although the flows themselves are produced in different ways). Second, the sizes of the vortices are physically comparable—they are determined by the Rossby scale, albeit by the two-dimensional radius r_R in our model and by the three-dimensional Rossby radius r_i in Hide's model.[30] It is not impossible that the further development of experiment and theory could give rise to a new model of large planetary vortices based on a synthesis of these models.

We thank V. K. Rodionov for assistance in the experiments and A. M. Fridman, A. V. Zhutoretskiĭ, and G. G. Sutyrin for fruitful discussions.

[1)]This estimate is correct provided that τ_{visc} is much greater than the period of intrinsic rotation of the vortex; in the case of the Red Spot this condition is satisfied (the intrinsic period is about a week) but in the experiments of Refs. 1 and 2 it is not; therefore, an estimate intermediate between (2) and $\tau_{visc} = H_0^2/\nu$ is evidently closer to the reality in Refs. 1 and 2.

[2)]We employ the expression *autosoliton*, following B. S. Kerner and V. V. Osipov, to designate a self-sustaining soliton which is undamped in a system with dissipation.

[3)]This improved model is evidently better described as a quasi-two-dimensional model.

[1]S. V. Antipov, M. V. Nezlin, E. N. Snezhkin, and A. S. Trubnikov, a) Pis'ma Zh. Eksp. Teor. Fiz. **33**, 368 (1981) [JETP Lett. **33**, 351 (1981)]; b) Zh. Eksp. Teor. Fiz. **82**, 145 (1982) [Sov. Phys. JETP **55**, 85 (1982)].

[2]S. V. Antipov, M. V. Nezlin, V. K. Rodionov, E. N. Snezhkin, and A. S. Trubnikov, Zh. Eksp. Teor. Fiz. **84**, 1357 (1983) [Sov. Phys. JETP **57**, 786 (1983)].

[3]V. I. Netviashvili, a) Pis'ma Zh. Eksp. Teor. Fiz. **32**, 632 (1980) [JETP Lett. **32**, 619 (1980)]; b) Pis'ma Astron. Zh. **9**, 253 (1983) [Sov. Astron. Lett. **9**, 137 (1983)].

[4]T. Maxworthy and L. G. Redekopp, Icarus **29**, 261 (1976); Science **210**, 1350 (1980).

[5]R. Z. Sagdeev, V. D. Shapiro, and V. I. Shevchenko, Pis'ma Astron. Zh. **7**, 505 (1981) [Sov. Astron. Lett. **7**, 279 (1981)].

[6]M. V. Nezlin, a) Pis'ma Zh. Eksp. Teor. Fiz. **34**, 83 (1981) [JETP Lett. **34**, 77 (1981)]; b) Pis'ma Astron. Zh. **10**, 530 (1984) [Sov. Astron. Lett. **10**, 221 (1984)].

[7]a) J. Pedlosky, Geophysical Fluid Dynamics, Springer, Berlin (1979), §4.12, Chap. 2 [Russian translation published by Mir, Moscow

(1984)]; b) P. H. LeBlond and L. A. Mysak, Waves in the Ocean, Elsevier, Amsterdam (1978) [Russian translation published by Mir, Moscow (1981)].
[8]a) B. A. Smith and G. E. Hunt, in: Jupiter (ed. T. Gehrels), University of Arizona Press, Tucson (1976) [Russian translation published by Mir, Moscow (1976)]; b) B. A. Smith *et al.*, Science **204**, 951 (1979); c) A. P. Ingersoll *et al.*, Nature **280**, 773 (1979); d) G. Hunt and P. Moore, Jupiter (ed. R. McNally) (1981), p. 96.
[9]P. B. Rhines, Ann. Rev. Fluid Mech. **11**, 401 (1979).
[10]a) G. P. J. Williams, J. Atmos. Sci. **36**, 932 (1979); b) G. P. Williams and T. Yamagata, J. Atmos. Sci. **41**, 453 (1984).
[11]M. V. Nezlin, E. N. Snezhkin, and A. S. Trubnikov, Pis'ma Zh. Eksp. Teor. Fiz. **36**, 190 (1982) [JETP Lett. **36**, 234 (1982)].
[12]S. V. Antipov, M. V. Nezlin, and A. S.Trubnikov, Pis'ma Zh. Eksp. Teor. Fiz. **41**, 25 (1985) [JETP Lett. **41**, 30 (1985)].
[13]S. V. Antipov, M. V. Nezlin, V. K. Rodionov, E. N. Snezhkin, and A. S. Trubnikov, Pis'ma Zh. Eksp. Teor. Fiz. **37**, 319 (1983) [JETP Lett. **37**, 378 (1983)].
[14]S. V. Bazdenkov and O. P. Pogutse, Pis'ma Zh. Eksp. Teor. Fiz. **37**, 317 (1983) [JETP Lett. **37**, 375 (1983)].
[15]L. D. Landau, Dokl. Akad. Nauk SSSR **44**, 151 (1944).
[16]L. D. Landau and E. M. Lifshitz, Mekhanika sploshnykh sred (Fluid Mechanics), Gostekhizdat, Moscow (1953) [Pergamon].
[17]a) V. L. Polyachenko and A. M. Fridman, Ravnovesie i ustoĭchivost' gravitiruyushchikh sistem (Equilibrium and Stability of Gravitating Systems), Nauka, Moscow (1976); A. M. Fridman and V. L. Polyachenko, Physics of Gravitating Systems, Springer, New York (1984); b) A. G. Morozov, Pis'ma Astron. Zh. **3**, 195 (1977); Astron. Zh. **56**, 498 (1979) [Sov. Astron. **23**, 278 (1979)].
[18]A. G. Morozov, M. V. Nezlin, E. N. Snezhkin, and A. M. Fridman, Pis'ma Zh. Eksp. Teor. Fiz. **39**, 504 (1984) [JETP Lett. **39**, 613 (1984)]; Usp. Fiz. Nauk **145**, 160 (1985) [Sov. Phys. Usp. **28**, 101 (1985)]; A. M. Fridman, A. G. Morosov, M. V. Nezlin, and E. N. Snezhkin, Phys. Lett. **109A**, 228 (1985).
[19]G. G. Sutyrin, Dokl. Akad. Nauk SSSR **280**, 1101 (1985).
[20]a) A. P. Ingersoll and P. G. Cuong, J. Atmos. Sci. **38**, 2067 (1981); b) A. Hatzes, D. Wenkert, A. P. Ingersoll, and G. E. Danielson, J. Geophys. Res. **86A**, 8745 (1981).
[21]Rayleigh, The Theory of Sound, Macmillan, London (1894), Chap. 21 [Russian translation published by GITTL, Moscow (1955)].
[22]G. R. Flierl, J. Phys. Oceanogr. **7**, 365 (1977).
[23]Ya. B. Zel'dovich and P. I. Kolykhalov, Dokl. Akad. Nauk SSSR **266**, 302 (1982) [Sov. Phys. Dokl. **27**, 699 (1982)].
[24]M. Rabaud and Y. Couder, J. Fluid Mech. **136**, 291 (1983).
[25]F. V. Dolzhanskiĭ, Izv. Akad. Nauk SSSR, Fiz. Atmos. Okeana **17**, 563 (1981); Yu. L. Chernous'ko, Izv. Akad. Nauk SSSR, Fiz. Atmos. Okeana **16**, 423 (1980).
[26]V. R. Eshleman, G. L. Tyler, G. E. Wood, G. F. Lindal, J. D. Anderson, and G. S. Levy, Science **204**, 976 (1979); R. Hanel *et al.*, Science **204**, 972 (1979).
[27]a) A. S. Monin and M. N. Koshlyakov, in: Nelineĭnye volny (Nonlinear Waves) (ed. A. V.Gaponov-Grekhov), Nauka, Moscow (1979), p. 258; b) V. M. Kamenkovich, M. N. Koshlyakov, and A. S. Monin, Sinoptichеskie vikhri v okeane (Synoptic Vortices in the Ocean), Gidrometeoizdat, Leningrad (1982).
[28]N. N. Romanova and V. Yu. Tseĭtlin, Izv. Akad. Nauk SSSR, Fiz. Atmos. Okeana **20**, 115 (1984).
[29]J. P. Dugan, R. P. Mied, P. C. Mignerey, and A. F. Schuetz, J. Geophys. Res. **87**, 385 (1982).
[30]P. L. Read and R. Hide, Nature **302**, 126 (1983); **308**, 45 (1984).

Translated by Julian B. Barbour